SCIENCE CHINA
Earth Sciences

• RESEARCH PAPER •

September 2016 Vol.59 No.9: 1854–1872
doi: 10.1007/s11430-016-5315-7

Extreme precipitation events in East China and associated moisture transport pathways

ZHAO Yang[1], XU XiangDe[1*], ZHAO TianLiang[2], XU HongXiong[1], MAO Fei[3], SUN Han[4] & WANG YuHong[1]

[1] *State Key Laboratory of Severe Weather, Chinese Academy of Meteorological Sciences, Beijing 100081, China;*
[2] *Collaborative Innovation Center on Forecast and Evaluation of Meteorological Disasters, Key Laboratory for Aerosol-Cloud-Precipitation of China Meteorological Administration, Nanjing University of Information Science & Technology, Nanjing 210044, China;*
[3] *Institute of Ecological Environment and Agricultural Meteorology, Chinese Academy of Meteorological Sciences, Beijing 100081, China;*
[4] *Guangxi Institute of Meteorological Disaster Mitigation, Nanning 530022, China*

Received November 16, 2015; accepted March 30, 2016; published online July 21, 2016

Abstract Interannual variation of summer precipitation in East China, and frequency of rainstorms during the monsoon season from 1961 to 2010, are analyzed in this study. It is found that the two variables show opposite trends on a decadal time scale: frequency of rainstorms increases significantly after the 1990s, while summer precipitation in East China decreases during the same period. Analysis of the spatial distribution of summer rainstorm frequency from 1961 to 2010 indicates that it decreases from the southeast to the northwest at the east edge of the large-scale topography associated with the plateaus. Spatial distribution of rainstorms with daily rainfall greater than 50 mm is characterized by a "high in the southeast and low in the northwest" pattern, similar to the staircase distribution of the topography. However, the spatial distribution of variation in both summer precipitation and frequency of extreme rainstorms under global warming differs significantly from the three-step staircase topography. It is shown that moisture characteristics of summer precipitation and extreme rainstorms during the monsoon season in East China, including moisture transport pathways, moist flow pattern, and spatial structure of the merging area of moist flows, differ significantly. Areas of frequent rainstorms include the Yangtze River Valley and South China. Column-integrated moisture transport and its spatial structure could be summarized as a "merging" of three branches of intense moist flows from low and middle latitude oceans, and "convergence" of column-integrated moisture fluxes. The merging area for moist flow associated with rainstorms in the high frequency region is located slightly to the south of the monsoonal precipitation or non-rainstorm precipitation, with significantly strong moisture convergence. In addition, the summer moist flow pattern in East China has a great influence on the frequency of extreme rainstorms. Moisture flux vectors in the region of frequent rainstorms correspond to vortical flow pattern. A comparison of moisture flux vectors associated with non-rainstorms and rainstorms indicates that the moist vortex associated with rainstorms is smaller in size and located to the south of the precipitation maximum, while the moist vortex associated with non-rainstorms is larger and located to the north. It is shown that column-integrated moist transport vortices and the structure of moist flux convergence have significant impacts on the north-south oscillation of frequent rainstorm areas in East China, which is synchronized with the maximum vorticity of moisture transport and the minimum of convergence on the decadal time scale. Synthesis of moisture transport pathways and related circulation impacts leads to a conceptual model of moisture flow associated with rainstorms.

Keywords Frequency of rainstorms, Moisture transport, Synoptic circulation, Extreme rainstorms, Synchronized variations, Vortex structure

Citation: Zhao Y, Xu X D, Zhao T L, Xu H X, Mao F, Sun H, Wang Y H. 2016. Extreme precipitation events in East China and associated moisture transport pathways. Science China Earth Sciences, 59: 1854−1872, doi: 10.1007/s11430-016-5315-7

*Corresponding author (email: xuxd@camscma.cn)

1. Introduction

China's climate is in general shaped jointly by the unique three-step staircase large-scale topography of the Tibet Plateau, and the East Asian Monsoon. During the monsoon season, frequent sustained regional heavy rainfalls often have severe consequences for both society and the economy. Tao (1980) showed that China is among the nations where summer rainfall can result in disasters because of monsoonal flow. Heavy rainfall events in China typically occur in the flooding season of May to August. Extreme rainfall in China is much higher than in other countries at the same latitudes. For example, the USA is also located in the same Humid Subtropical Climate zone as China; but the duration of rainfall is longer in China, and the affected area is significantly greater. Liu et al. (2009) showed that summer precipitation and rainstorms in China are related to both the Indian monsoon and the western Pacific summer monsoon flow. They found that, during the last 75 years (1931–2006), there were at least 5 recorded extreme precipitation events in which the total rainfall reached or exceeded 1000 mm within 24 hours. These extreme events last from a few hours to 63 days. For example, the duration of the 1896 event was 65 days. During the 1954 and 1998 heavy rainfall events, more than 600 mm of rain fell over the majority of the Yangtze River area.

Wang et al. (2002) showed that during the 1980s, there were 6 years in which the climate of China was characterized by a distinct pattern of flooding in the Yangtze River and drought in Northern and Southern China, and the frequency of this climate pattern was 4 times the climate mean (14.5%). Wang et al. (2002) also found that the climate of China co-varies with global climate over land to a great extent, except that in China, the decadal variation in precipitation is more pronounced while in global precipitation the long term trend is stronger. Two prominent spectral peaks emerged from China's precipitation record: at 3.3 and 26.7 years. The former is likely due to ENSO. The latter is related to decadal variation in precipitation in China, and this is probably due to decadal variation of climate rather than the global climate trend. Some authors (Tao et al., 1988; Si et al., 1996) found that the rain bands in the middle and lower reaches of the Yangtze River Valley are related to the strength of the summer monsoon, which indicates that the East Asia Monsoon is a key factor determining the Meiyu system in East China and its latitudinal variations, and that meridional winds play an important role in the drought/flooding pattern in China. Decadal variation of the East Asian summer monsoon (EASM), and its mechanism, has become a research focus in recent years. Guo et al. (2003) showed that the amplitude of the EASM has weakened twice since the middle of the 20th century. The first weakening of the EASM occurred in the mid-1960s, and the second in the mid1970s, after which it EASM has remained weak. During periods of enhanced EASM, East China is anomalously wet in the north and dry in the Yangtze River area, while western China is wet in the south and dry in the north. The dry/wet pattern reverses during periods of weakened EASM. These past studies, however, do not answer some important questions: What is the decadal variation in the spatial and temporal distribution of rainstorm frequency? How does it relate to precipitation variation in the EASM? How do the inter-annual and decadal variations of rainstorm frequency relate to the three-step staircase topography of the Tibet Plateau?

From the point of view of moisture origins, Xu et al. (2013) showed that Tibet, the Indian Ocean, the Bay of Bengal, and the South China Sea are important moisture source regions, all contributing to the rainfall anomalies in China. The main source of water vapor in the Yangtze River Valley in summer is the western Pacific and South China Sea. The Indian Summer Monsoon and South China Sea Summer Monsoon are primarily responsible for the transport of water vapor to the Yangtze-Huaihe River Valley (Zhou et al., 2005). Major water vapor sources for rainfall in East China are, in descending order of importance, the South China Sea, Bay of Bengal, and western Pacific (Sheng et al., 1981; Chen et al., 1982; Jin, 1981). Chen et al. (1991) showed that the external water vapor sources for summer rainfall in mainland China are the South China Sea, the southwest monsoon from the Bay of Bengal, and the southeast monsoon of the subtropical plateau. Simmonds et al. (1999) argued that China has two major regions of rainstorms. Water vapor is transported into China from the southern and western boundaries, and transported out at the eastern boundary. The southern boundary is considered to be the main water vapor pathway for rainstorms in the southern region, and the western boundary for rainstorms in the northern region. Tao et al. (1994) performed numerical experiments for the rainstorm of July 10–11, 1991 in the Yangtze-Huaihe River Valley. They showed that water vapor transport from the Bay of Bengal via southwest monsoon flow contributed more to the rainfall than that from the South China Sea via southeast monsoon flow, and nonlinear interaction and mutual enhancement occurred in the presence of both water vapor pathways. Chow et al. (2008) showed that the main water vapor pathway for the early summer rainfall in China is through the southwest Indian Monsoon flow; a weak Indian Monsoon leads to a dry anomaly (e.g., the reduced rainfall period in 1992); an active Indian Monsoon, on the other hand, leads to flooding (e.g., the 1998 rainstorms in the Yangtze River Valley). Overall, monsoon flow dominates over China, and the transport of moisture by the summer monsoon flow plays important roles in the summer rainstorms. The moisture transport in East China has been documented by many authors. It is nevertheless not fully understood how it relates to the moisture sources of monsoon rainfall, moisture pathways, and moisture circulation patterns.

There is no doubt that improved understanding of extreme

rainstorm frequency and its inter-annual and decadal variations, as well as the factors controlling them, is of great strategic value for informing disaster prevention and mitigation. The status of the knowledge is that the spatial and temporal characteristics of extreme rainstorm events in China and the key factors contributing to them are highly complex; much uncertainty remains despite decades of research, and many prominent questions have yet to be addressed. For example, why do regions of high-frequency rainstorms in China, in comparison to similar climate zones or similar latitudes, have higher extreme rainfall values, larger impact areas, and greater durations? How do low latitude oceanic moisture sources transported via certain pathways under the influence of the East Monsoon and the great Tibet terrain structure, together with its closely-related circulation pattern, determine the unique spatial distribution of frequent rainstorms in China? What is the main difference between the extreme rainstorms in East China and summer rainfall, in terms of trend, and spatial and temporal patterns? Is there any relationship between the extreme regional rainstorms and the spatial and temporal patterns of the summer Meiyu systems? To what extent do the two share the same characteristics, or differ in the structure and characteristics of the sustained hydrological cycle? What is the impact of variations in moisture transport by the East Asia Monsoon on the spatial and temporal patterns of rainstorm frequency in East China and its inter-annual and decadal variability?

2. Data and methods

This study uses the following NCEP/NCAR reanalysis datasets: monthly mean winds and specific humidity fields (2.5°×2.5°) and daily mean specific humidity fields (1°×1°) from 1961 to 2010. Based on precipitation data collected from a total of 601 surface meteorological observation stations with rainfall records from 1961 to 2010, the number of days from July to August over which rainstorms have precipitation less than 50 mm, or exceed 50, 100, and 200 mm, and the number of days of non-storm precipitation (i.e., light rain, moderate rain, and heavy rain) are used to compute statistics. These 601 stations largely cover the whole of mainland China except that they are scattered in the plateau area. Thus, collectively they are representative of the spatial and temporal distribution of rainstorms over most of China. These data will be used to study the inter-annual and decadal variability of water vapor during rainstorms, and the relationship between moisture transport and rainstorm areas.

2.1 Method for computation of Column-integrated water vapor fluxes

The study focuses on the relationship between the frequency of rainstorms and water vapor transport. We use the following equations to compute *qu* and *qv*, column-integrated horizontal water vapor fluxes in the zonal and meridional directions, respectively:

$$qu = \frac{1}{\mathrm{g}}\int_{p_s}^{p_T} qu\mathrm{d}P\,, \tag{1}$$

$$qv = \frac{1}{\mathrm{g}}\int_{p_s}^{p_T} qv\mathrm{d}P\,, \tag{2}$$

where g is gravity, u and v are the zonal and meridional wind components, respectively, q is specific humidity, p_s is surface pressure, and p_T is the pressure at the top of the atmosphere.

2.2 Correlation vector

To elucidate the relationship between rainstorms in East China and column-integrated water vapor transport, and particularly the role of moisture transport during the years of anomalous rainstorms, we compute the correlation vector, $\vec{R}(x, y)$, to track water vapor sources and transport pathways. $\vec{R}(x, y)$ is defined as

$$\vec{R}(x, y) = \vec{i}R_u(x, y) + \vec{j}R_v(x, y)\,, \tag{3}$$

where $R_u(x, y)$ and $R_v(x, y)$ represent correlation coefficients between the frequency of rainstorms or rainfall and column-integrated zonal/meridional water vapor fluxes *qu* and *qv*, respectively (Xu et al., 2008).

2.3 Modeling with FLEXPART (Particle dispersion model)

The FLEXPART model is adopted to compute spatial and temporal variations of water vapor transport pathways in the rainstorm area over the Yangtze River Valley. FLEXPART was developed at the Department of Atmospheric and Climate Research, the Norwegian Institute for Air Research (Stohl et al., 2005). As a Lagrangian transport and dispersion model, FLEXPART is suitable for tracking the history of atmospheric tracers. FLEXPART is also capable of computing the tracks of air particle clusters to infer processes of atmospheric transport and dispersion. This study uses FLEXPART to compute backward trajectories in the rainstorm areas. The NCEP FNL 1°×1° analysis dataset is used to drive FLEXPART. The initial positions of particle clusters are in the middle and lower reaches of the Yangtze River (118.25°–123.5°E, 28.5°–33.25°N), from 100 to 6000 meters altitude. The computation period is between June 1 to June 12, 2008.

2.4 Other methods

In addition to the above methods, we also used the following

computations: variations, correlation coefficients, normalization, multiple linear regression.

3. Seasonal and decadal variations in rainstorm frequency in East China

Consider the frequency of rainstorms in East China (east of 150°E). We have computed the annual frequency of rainstorms in each month with precipitation between 50–100 mm (Figure 1a), >100 mm (Figure 1b), and >200 mm (not shown). Monthly mean frequencies of the rainstorm categories show that there is a significant difference in the rainstorms in each category; the frequency of rainstorms in all categories reaches a peak in the summer. The summer is also the season of the heaviest rainstorms, and the >50 mm category is the key category.

In synoptic meteorology, a rainstorm is defined as a precipitation event with daily precipitation reaching or exceeding 50 mm. Rainstorm climatology research shows that in China, rainstorms mainly occur east of 105°E. Due to complex multiple-scale interactions among monsoonal, Meiyu, typhoon, subtropical high, cyclonic, and mesoscale convective systems under the influence of the Tibet Plateau and Loess Plateau, there are substantial regional and seasonal disparities in rainstorm distribution in China.

Some studies have shown that there is a close relationship between the three-step staircase topography (Figure 2a) and northward migration of the Meiyu system in the summer. It has been shown that seasonal variations in land-atmospheric processes in the Tibet Plateau and the Loess Plateau "thermodynamically drive" or "dynamically pull" the Meiyu rainbands from their initial position in the southeast coastal areas to the northwest, where

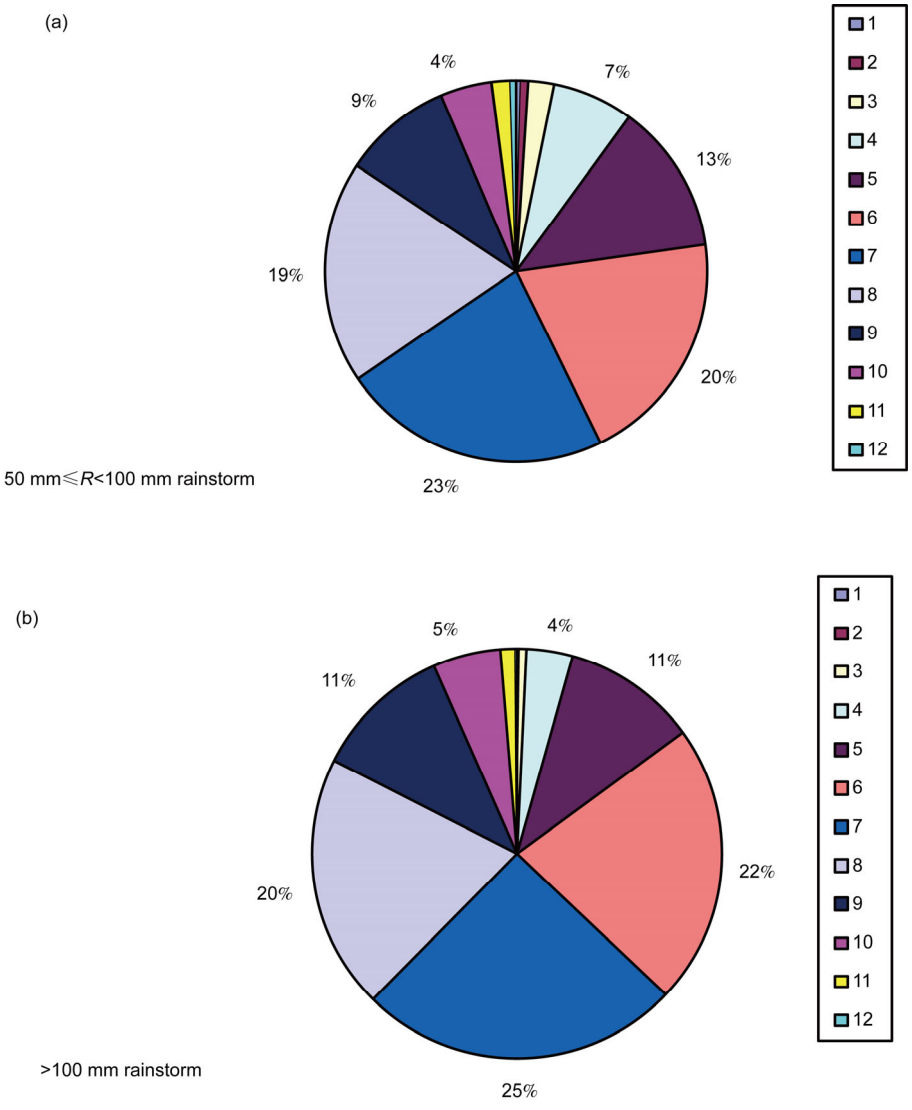

Figure 1 Monthly fractions of rainstorm frequency over East China; with daily precipitation (a) 50 mm≤R<100 mm; and (b) R≥100 mm. Filled colors indicate proportions of rainstorms in each month of the year.

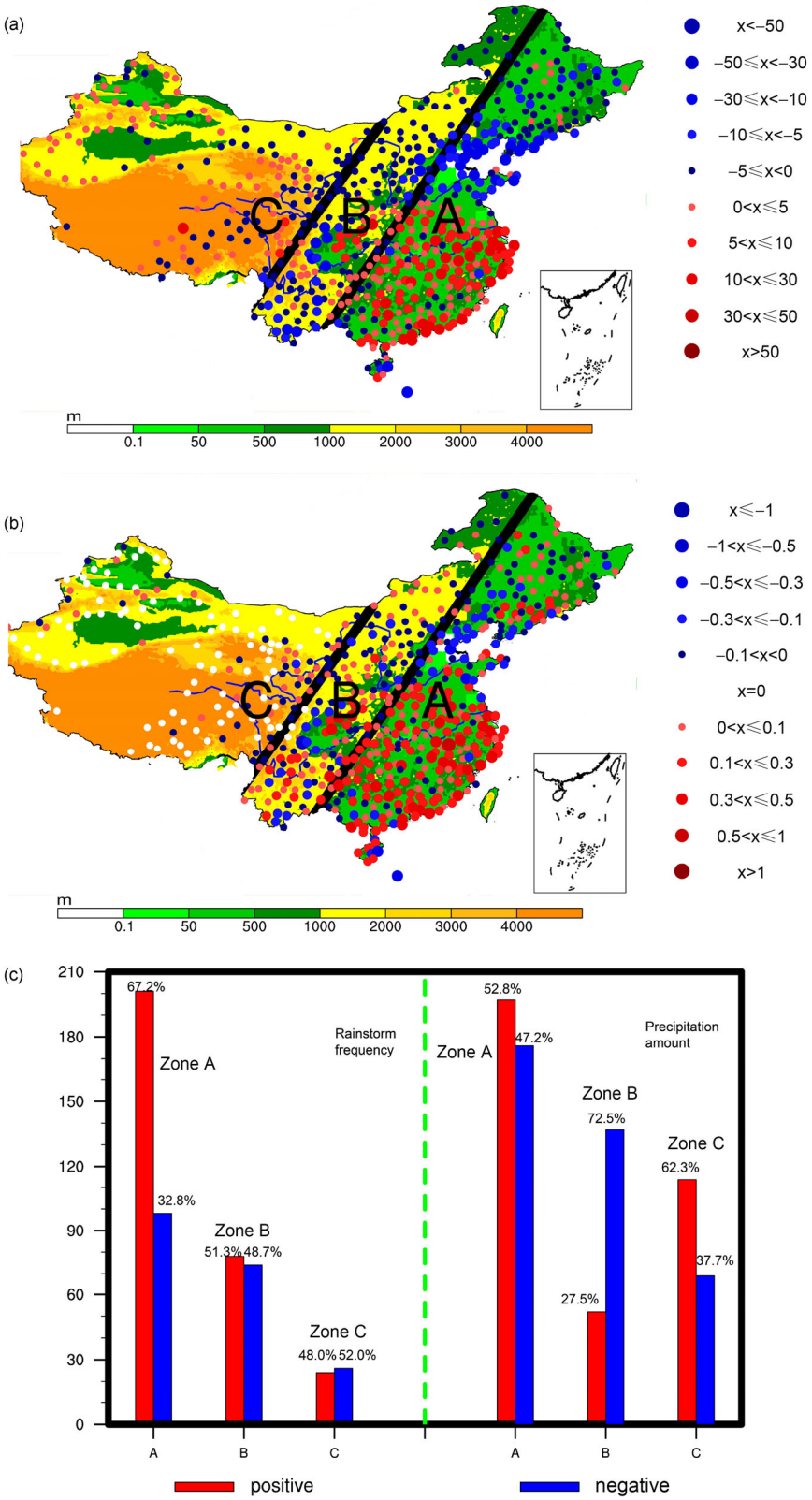

Figure 2 Decadal trends in summertime precipitation (a) and rainstorm frequency (b) from 1961–2010 in mainland China, and comparison of the number of stations with positive and negative interannual variation trends over three regions (c). Altitude of the large-scale topography is color-shaded. A: plains over East China; B: between the East China plain area and the plateaus; C: West China.

they subsequently remain stationary (Figure 2a) near the "topographical line" at the edge of the plateaus (Xu et al., 2000).

On seasonal or monthly time scales, summer precipita-

tion in East Asia shows several distinct rain bands. Hence, it is important to study the relationship between the monsoon and precipitation separately in these regions: South China, North China, and the Yangtze-Huaihe River Valley (Liu et al., 2004). Our computation of the frequency of summer rainstorms from 1961–2010 also shows that the frequency of rainstorms in East China is higher in the southeast and lower in the northeast, which is very similar to the distribution of the "staircase" topography. The similarity in the pattern of the three-step staircase topography and the rain bands suggests a strong link between the rainstorm frequency and seasonal migration of the Meiyu front, moisture transport by monsoonal flow, and the dynamic and thermodynamic influence of large-scale topography. One may also ask if there is a relationship between the frequency of rainstorms in space and time and interannual variation in summer precipitation. Bao et al. (2006) found that summer rainstorms have significant decadal variations: the number of rainstorm days in the Yangtze-Huaihe River Valley increased in the 1970s and late 1980s; rainstorm frequency in South China also showed strong decadal variations. Liu (1999) showed that both the number of extreme rainstorm days and the amplitude of rainstorms increased after the 1980s, except in North China.

The Intergovernmental Panel on Climate Change (Church et al., 2014) reported that global and regional hydrological cycles have undergone significant changes over the past century. Wang (2001) showed that the precipitation pattern in East China is closely related to the decadal weakening of the East Asia Summer Monsoon, which has periods of 1 year and 60–80 years. The primary precipitation pattern during the Meiyu period is that the precipitation anomaly in the Yangtze River Valley is out of phase with that in South China, while precipitation south of the Yangtze River is in phase with most other areas (Ma et al., 2012). Figure 2a shows the decadal variation of summer precipitation across mainland China. Considering that total precipitation is different from extreme rainstorms, we further compute spatial distribution of rainstorms in East China (Figure 2b). Figure 2a displays the well-known pattern of "flooding in the south and drought in the north" in the East China summer (zone A), and the number of stations with positive interannual variation is similar to the number of stations with negative variation in zone A (right panel of Figure 2c); in Western China, however, the positive rate of interannual variation dominates; i.e., the number of stations with positive interannual variation is greater than the number of stations with negative variation. Besides, a majority of stations show negative interannual variation in the northeast-southwest oriented precipitation bands (Figure 2a). Comparing Figures 2a and 2b indicates that decadal variabilities in summer precipitation and frequency of rainstorms (daily precipitation greater than 50 mm/day) in China have different spatial distributions. From the variation in the frequency of rainstorms (Figure 2b), stations in the Tibet Plateau and plain area to the east of the Loess Plateau, South China, the Yangtze-Huaihe River Valley, Central China, Northern China, and northeast China show a southwest-northeast oriented banded pattern with significant positive precipitation variations, and the number of positive variations is about twice the number of negative variations (left panel of Figure 2c). Figure 4b shows that the area discussed above (Figure 2b) coincides with the high frequency region for summer rainstorms with daily rainfall greater than 50 mm. This indicates that the risk of a rainstorm disaster in the Yangtze River and south of the Yangtze River already shows a significant increasing trend. In addition, east of the large-scale plateau topography and the transition area to the plain there is a large area of positive variation in the frequency of rainstorms (Figure 2b), and the number of stations with positive variation is similar to the number of stations with negative variation (left panel of Figure 2c). Note that the area south of 30°N in East China has significant positive decadal variations in both the summer rainfall and frequency of rainstorms. In addition, areas of positive variation in rainstorm frequency are the same as those with high mudslide frequencies, in the transition area of steep terrain between the high-altitude topography and the plain area. For example, the Yunnan-Guizhou Plateau shows significant positive variation in the rainstorm frequency, which coincides with a south-north oriented band of high frequency of mudslides and mountain flood disasters east of the Tibet Plateau. Therefore, the frequency of the extreme rainstorms generally increases in East China, and this poses a great challenge to the implementation of risk reduction and disaster prevention in areas of high mudslide frequency and mountain flooding. The precipitation variation in East China shows the pattern of "flooding in the south and drought in the north", and in West China shows an increasing trend in precipitation. This result is consistent with prior studies. The transition zone from the Tibet Plateau to the plain area is dominated by negative variation; and the frequency of rainstorms gradually decreases from the southeast high-frequency zone to the northwest zone with high-altitude topography. The primary characteristic of rainstorms with daily precipitation more than 50 mm is a distribution "high in the southeast and low in in the northeast", similar to the staircase pattern of the terrain, and also similar to the orientation of the periphery of the Meiyu system. The Tibet Plateau and Loess Plateau overall have some fraction with increasing frequency of rainstorms, and positive variations in the northeast of these areas. In the plateau area and the transition zone to the plain, variation in the frequency of rainstorms differs from variation in summer precipitation, and shows some signs of increase (similar positive and negative trends). The frequency of mudslides increases here, while there is no apparent trend in the west.

Based on the spatial and temporal distribution of rainstorm frequency (with daily precipitation >50 mm), the present study finds that it is appropriate to define the rela-

tively concentrated area of rainstorms in East China as the area east of 105°E. Our discussion below is based on this definition. It is found that interannual variation in the summer precipitation and extreme rainstorms (with daily rainfall more than 50, 100 and 200 mm) differ significantly. Our calculation shows that rainstorms of these three categories occurred less frequently in East China from the 1960s to the 1980s; however, since the 1990s, there is an increasing overall trend with more fluctuations. A comparison of interannual variation in summer rainstorms and precipitation shows that there is a substantial difference in the phase of the two quantities from 1961 to 2010, and their interannual variation has the opposite trend; the former shows an increasing trend in the frequency of rainstorms with daily rain more than 50 mm from 1961 to 2010, while the later shows a decreasing trend in the total summer precipitation in East China (Figure 3).

4. Meridional transport of moisture by the summer monsoon and decadal variability in rainstorm frequency in East China

As discussed in the introduction, the low latitude Meiyu system and its northward migration in East China, as well as the interannual variation in the East Asia Monsoon, are critical factors. The meridional transport of moisture in summer is closely related to the regional distribution of flooding and drought in China (Tao et al., 1988; Shi et al., 1996). Considering that the areas of frequent rainstorms in South China are closely related to the structure of moisture transport by monsoonal flows, and an area of concentrated frequent rainstorms is the south of the Yangtze River, and south of 30°N, we will analyze the interannual variation in the column-integrated moisture transport to the east of 105°E, 20°–45°N. In addition, we will also analyze the interannual variation of anomalous values in column-integrated moisture south of 30°N in East China.

A comparison of the decadal variation in column-integrated moisture in south China and the meridional flux of column-integrated moisture (Figure 4a) indicates that the decadal variation in moisture flux between 20°–45°N shows a weakening trend. Column-integrated moisture flux in East China reached a peak in the 1960s, and shows a decreasing trend afterwards, corresponding to the pattern of summer rainstorm frequency (Figure 4bA); i.e., the pattern of the anomaly is oriented southwest-northeast in the northeast, Inner Mongolia, Shanxi, and east of the plateau areas. The decreasing trend continues in the 1970s, and the frequency of summer rainstorms is similar to that of the 1960s (Figure 4bB); i.e., North China has a southwest-northeast oriented band with positive anomalies. Column-integrated moisture flux shows a gentle decrease in the 1980s, when it reached a minimum. The corresponding distribution of summer rainstorm frequency shows positive anomalies in the middle and lower reaches of the Yangtze River with an east-west oriented band. In the 1990s, the column-integrated moisture flux continued to maximize in the trough, but fluctuated greatly; correspondingly rainstorm frequency had positive anomalous values in the Yangtze-Huaihe River Valley in East China and South China (Figure 4bD). In the first 10 years of the 21st century, the column-integrated moisture flux recovered from the minimum and increased slowly. Correspondingly two east-west oriented bands emerged in the Yangtze-Huaihe River Valley and South China, in between which a negative anomaly oriented east-west can be found (Figure 4 bE). Overall, the north-south shift in the frequent rainstorm areas varies in phase with column-integrated moisture flux in the decadal time scale. In the years of greater summer column-integrated moisture fluxes in East China, the frequent rainstorm areas shift to the north; and conversely, in the years of lesser summer column-integrated

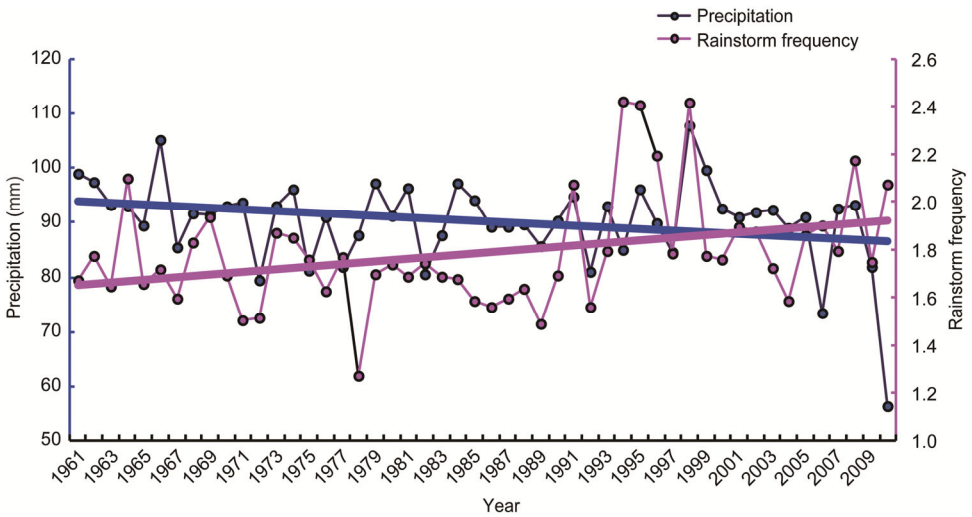

Figure 3 Interannual variations (lines with point markers) and trends (straight lines) in summer precipitation (blue; correlation coefficient is –0.273 and trend is –0.1493 per year) and rainstorm frequency (purple; correlation coefficient is 0.337 and trend is 0.0055 per year) over East China.

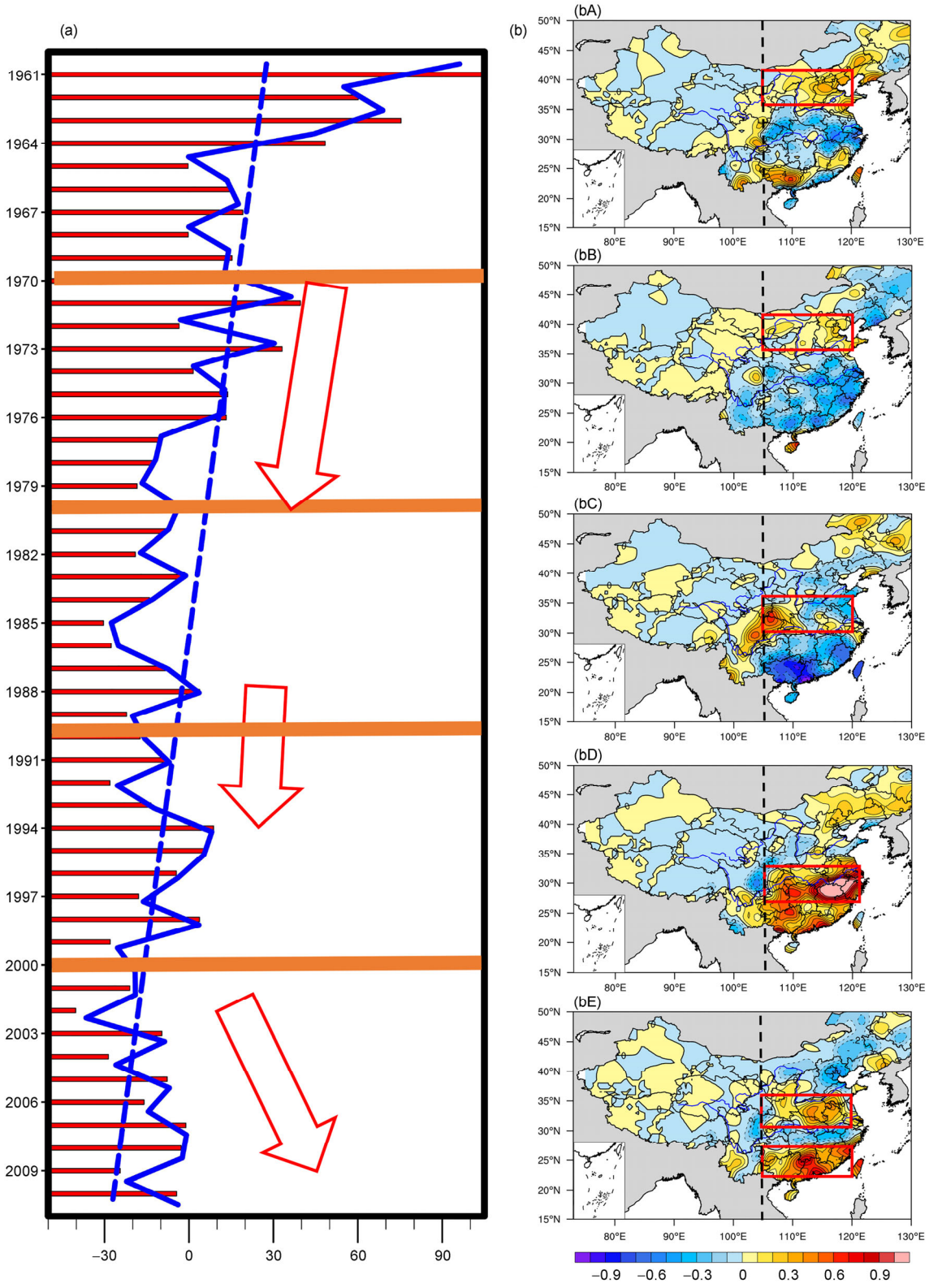

Figure 4 Decadal anomalies from 1961 to 2010 in the summertime column-integrated moisture transport (g cm^{-1} s^{-1}) averaged over the region (105° to 120°E; 20° to 45°N) (a), and distribution of decadal anomalous rainstorm frequency in East China (b). (bA) the 1960s, (bB) the 1970s, (bC) the 1980s, (bD) the 1990s and (bE) the 2000s.

moisture fluxes in East China, the areas of highly frequent rainstorms shift to the south. The relationship between the two suggests that a north-south shift of the region with frequent rainstorms can also modulate the strength of column-

integrated moisture fluxes. Our results on column-integrated moisture fluxes and the spatial and temporal characteristics of rainstorms are consistent with those of Liu et al. (1999) on the decadal variation of rainstorm frequency in South China, the Yangtze-Huaihe River Valley, North China, and Northeast China.

5. Relationship between extreme rainstorms in East China and moisture fluxes

Prior to the onset of the monsoonal flow, the timing of heavy precipitation is very similar to the timing of mid-latitude moisture transport by westerlies; after the onset, timing of the heavy precipitation is similar to moisture influx in the southern boundary carried by southerlies in the South China Sea. Because southwesterlies strengthen after the onset of the SCS Monsoon, moisture transport to the southwest boundary of South China increases substantially (Zhao et al., 2015). These results indicate that the change of monsoonal flow and regional atmospheric circulation pattern can lead to moisture transport from ocean to land, set up large-scale convergence/divergence of moisture, and further cause regional heavy precipitation and extreme rainstorm events. Our study also indicates that there is a statistically significant relationship between decadal variation in the frequency of summer rainstorms in the south of East China and the strength of meridional moisture flux during the monsoon season (Figure 4a and 4b). We will further analyze the spatial distribution of moisture transport that strongly influences the rainstorm frequency in East China. Summer precipitation in East China, the frequency of rainstorms (daily precipitation greater than 50 mm) and the correlation vector of column-integrated moisture transport were computed and are shown in Figure 5. Figure 5a indicates that the area of concentrated summer Meiyu precipitation covers the Yangtze River and the majority of the area to the south of the Yangtze River, characterized by the dipolar pattern of "rich in the south and poor in the north". Corresponding to this precipitation pattern is the convergence of the transport of moisture by westerlies and by the three branches of moisture transport by monsoonal flows (the Indochina Peninsula, the Bay of Bengal, and the South China Sea), and the convergence zone of these multiple moisture transport pathways shifts to the north with the maximum located in the Yangtze-Huaihe River Valley. From the correlation vector between column-integrated moisture fluxes (*qu* and *qv*) and frequency of rainstorms in East China, one can see that column-integrated moisture transport shows "merging" characteristics in the area of concentrated frequent rainstorms in the Yangtze River Valley and South China. This includes one branch of the pathway, which transports moisture from the northeast to southwest along the eastern side of the Tibet Plateau and Loess Plateau, making a "big bend" and deflecting to the east at the southeast border of the Tibet Plateau, then merging with the southwest moisture transport pathway from the southwesterlies in the Bay of Bengal and intense moisture transport in the South China Sea. The merging moisture transport pathways eventually reach South China and the Yangtze River Valley. The convergence of the column-integrated moisture transport pathways is located slightly to the south of the summer precipitation pattern. Of particular interest is the region of frequent rainstorms along the east edge of the plateau, covering the majority of the plain area, where the moisture transport from south to north reaches a maximum in several areas, including in the south of the Yangtze River Valley and South China. This constitutes the key "supply chain" for moisture to the region of frequent rainstorms in East China. The total amount of summer precipitation reaches a maximum in South China, which does not overlap with the maximum of the moisture transport (in the Yangtze-Huaihe River Valley). Moisture transport in the region of frequent rainstorms reaches a maximum in the Yangtze River Valley and to the south of it; so the two overlap. Figure 5b shows that the plain area to the east of the Tibet Plateau and Loess Plateau has frequent rainstorms (with daily precipitation >50 mm). Among them, the Yangtze River Valley and South China (Zone A) and the Sichuan Basin are concentrated areas of high rainstorm frequency. Immediately east of the plateaus (Zone B) there are somewhat fewer rainstorms relative to East China, as is also the case in the northwest region (Zone C). The comprehensive analysis above shows that variation in the total summer precipitation in East China is structurally different from the moisture pathways related to rainstorms. Therefore, it is of unique scientific value, and practical significance to forecasting, to study the spatial and temporal variations in the frequency of extreme rainstorms.

Analysis of correlations between the frequency of summer rainstorms in East China and column-integrated moisture fluxes (Figure 6a) shows signs of moisture convergence (negative divergence) in the middle and lower reaches of the Yangtze River and South China (Zone A). When flux convergence in the column-integrated moisture transport in East China is enhanced, moisture transport originating from low latitude ocean shows "permanent convergence", providing sustained abundant moisture to facilitate the development of extreme rainstorms in East China. The enhanced moisture flux convergence is therefore a key factor for understanding rainstorms in East China. The correlation coefficient between interannual variation of the frequency of rainstorms in East China and column-integrated moisture flux convergence reaches –0.497, indicating high correlation (Figure 6b).

We select the years with high and low values of negative correlation between the frequency of rainstorms and moisture flux convergence (Zone A) for composite analysis (i.e., anomalously lower moisture convergence [negative divergence] in 1961, 1963, and 1967; and anomalously higher

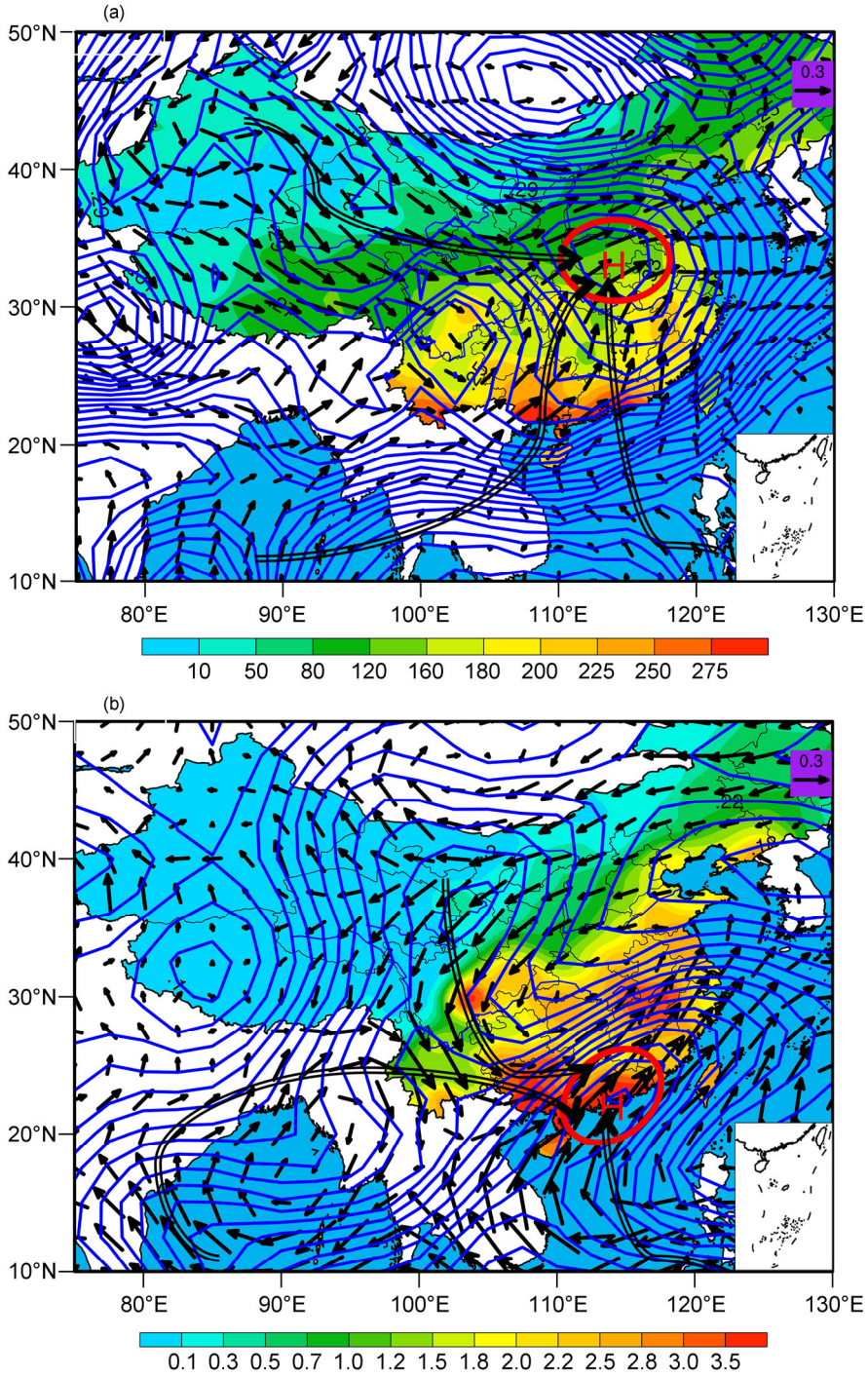

Figure 5 Distribution of rainstorm frequency with daily precipitation >50 mm; (a) summertime precipitation (unit: mm/d with average values shaded in color, and correlation vectors of column-integrated water vapor transport fluxes (unit: g s^{-1} hPa^{-1} cm^{-1}); (b) from 1961–2010. The red circles indicate high correlations.

moisture divergence in 1994, 1997 and 1998). A comparison of the geopotential height, temperature and column-integrated moisture transport (Figure 6c and d) indicates that during the years of frequent rainstorms, high values are found at a pressure of 500 hPa in the middle west and the Tibet Plateau. This corresponds to the moisture flux to the northwest of 30°N over the Tibet Plateau, which merges with the southwest moisture flux from the Bay of Bengal and South China Sea slightly south of 30°N, and coincides with the region of frequent rainstorms in the south of Yangtze River Valley. In addition, the moisture flux convergence is located slightly to the north of the rainstorms (about 30°–40°N) during the years of when rainstorms are less frequent.

The moisture flux convergence shifts to the north during

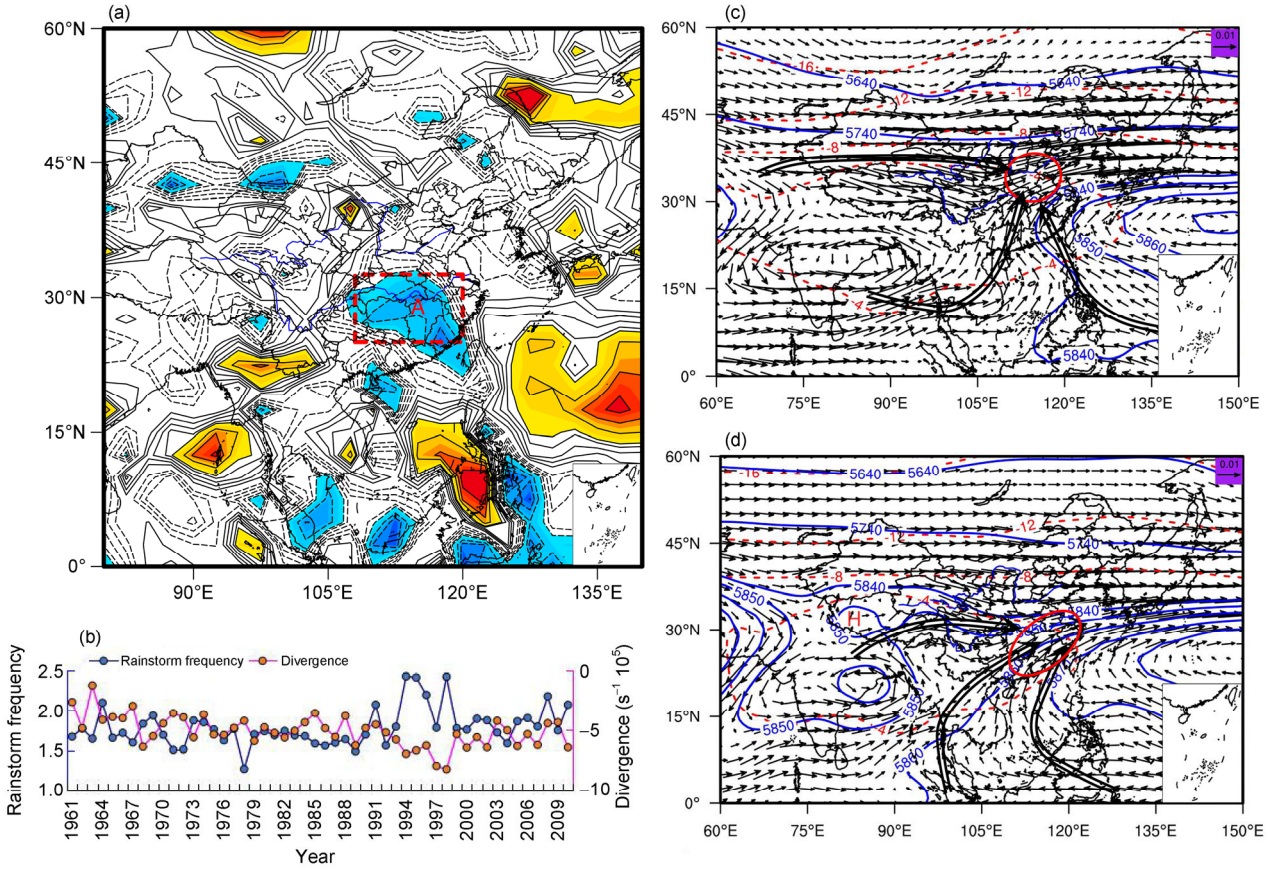

Figure 6 Correlation analysis of rainstorms in East China and column-integrated moisture flux divergence over East Asia. (a) correlation coefficient distribution; (b) interannual variations of column-integrated moisture flux divergence (unit: g s^{-1} cm^{-2} hPa^{-1}, red) and the frequency of rainstorms (blue); (c) and (d) geopotential height temperature (°C), and moisture transport flux (unit: g s kg^{-1}) at 500 hPa in years of anomalously low and high moisture transport flux divergence. Note that the square in Figure 6a indicates high correlation (convergence of moisture fluxes), and the red circles in Figure 6c and d denote the "convergence zone" of moisture transport. The open arrow indicates the primary direction of the column-integrated moisture transport pathway and moisture fluxes.

years of anomalously low moisture transport, while it shifts to the south in the south of the Yangtze River Valley during the years of anomalously high moisture transport. The above analysis indicates that the north-south oscillation in the convergence of the three branches of the moisture transport pathways corresponds to anomalously higher and lower frequencies of extreme rainstorms. From the circulation setup in geopotential height and temperature (Figure 6 c and d), the strength of the Tibet high at 500 hPa is very likely the key factor determining the north-south oscillation in the convergence of the three branches of moisture transport pathways.

The above results suggest that the thermodynamic structure of the Tibet Plateau may strongly influence the frequency of extreme rainstorms in East China, by modulating the north-south shift in the convergence of the three moisture transport pathways.

To gain further insight into the correlation between the moisture flux convergence and rainstorms in East China, we computed the interannual variations in the correlation between the convergence and frequency of rainstorms. This analysis indicates that the frequency of rainstorms and high and low values of sensitivity factors are in the opposite phase. Therefore the scatter plot (not shown) of regions of high moisture convergence and rainstorm frequency in East China shows a negative correlation between the frequency of rainstorms and column-integrated moisture flux convergence (at significance level of 1%).

6. A conceptual picture of the oceanic moisture sources of rainstorms in East China, and vortex patterns of moisture transport

The above results indicate that moisture fluxes, and their convergence and dynamical structure, have a definite impact on rainstorms in East China. The next question is to understand characteristics of the moisture transport during extreme rainstorms under the influence of the summer monsoon. It is also necessary to discriminate the pattern of moisture transport for rainstorms and monsoon precipitation for various categories of rainfall, e.g., rainstorms, torrential

rain, and regular rain (light, moderate, and heavy rain). Tian et al. (2012) discussed three categories of summer rainfall, and its relationship to anomalous moisture transport, and showed that the central rain belt corresponds to the merging of two anomalous moisture transport pathways in the Yangtze River, one from the northeast in East China and the other from the southwest. The southern rain belt corresponds to the merging of two anomalous moisture transport pathways in South China: one from the northeast and the other from the southwest in the northwest side of the subtropical North Pacific High. The northern rain belt corresponds to the merging of two anomalous moisture transport pathways in North China: one from the mid-latitude upstream by westerly transport and the other from the southwest in the northeast side of the subtropical high. The weather systems producing rainstorms in China include tropical cyclones, regional vortices and lows, frontal cyclones, typhoons and typhoon residuals. The onset and development of these systems are closely related to multiscale interactions under the influence of various large-scale circulation patterns. For rainstorms in East China, moisture transport and related circulation patterns are apparently key factors to consider.

Based on the rainstorm frequency and various rainfall events from 1961 to 2010, our analysis indicates that moisture transport is characterized by a large-scale cyclonic correlation vector, impacting the majority of East China, which will be referred to as the moisture transport vortex in the rest of this paper. We will discuss how the strength of the moisture transport vortex "drives" the transport of oceanic moisture in the low latitudes to East China. Figure 7 shows the frequency of the summer rainfall events with daily precipitation below 50 mm (including light, moderate, and heavy rain) and moisture fluxes in East Asia. Figure 7a and b use the frequency of rainfall events below 50 mm and the correlation vector of moisture transport as the background. The filled areas indicate regions of high correlation vector

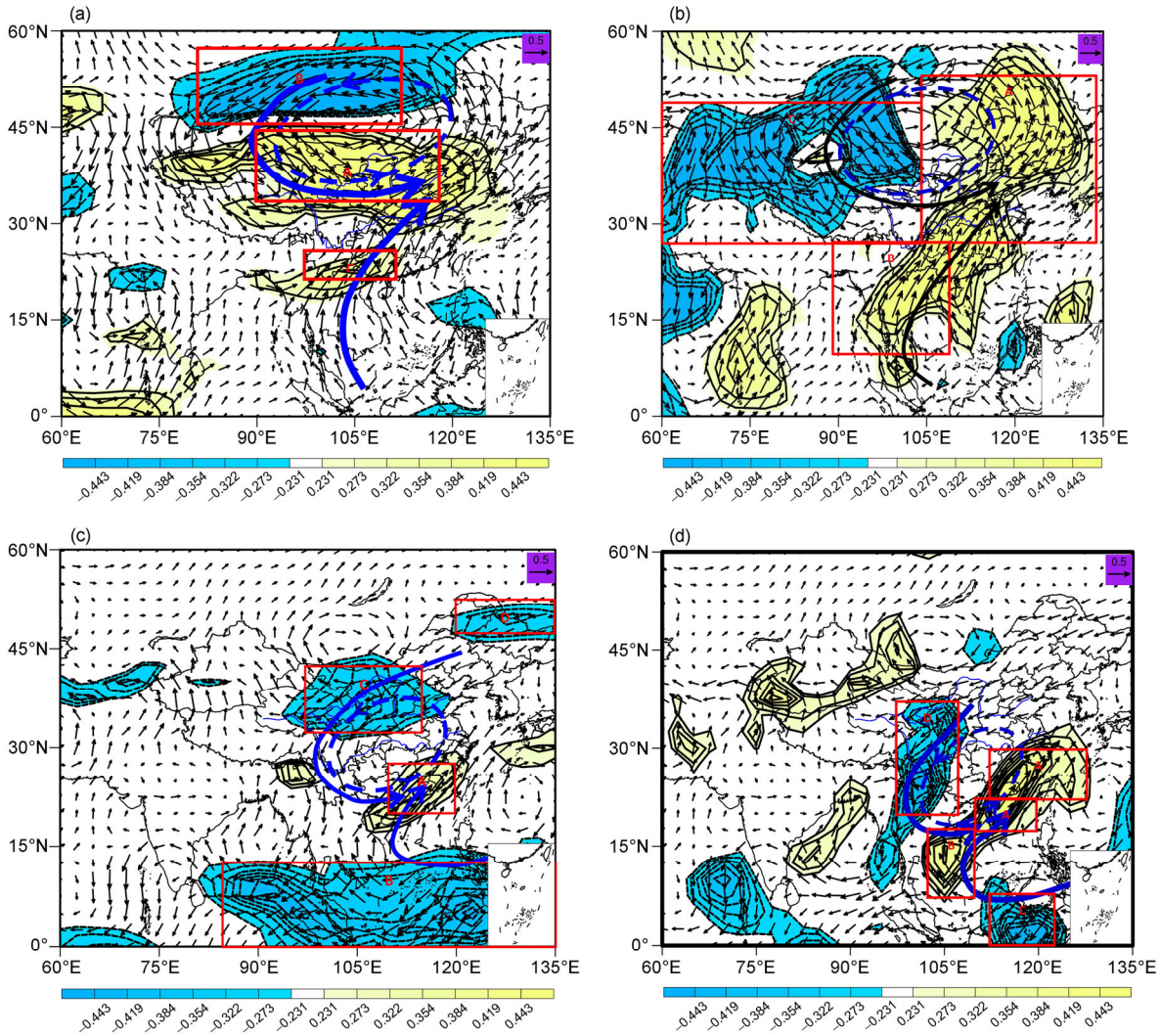

Figure 7 The correlation vectors for the frequency of regional averaged light-rainstorms (daily precipitation <50 mm) in East China and column vapor transport flux. (a) zonal and (b) meridional components (color shaded, unit: g s^{-1} hPa^{-1} cm^{-1}). (c) and (d) are the same as (a) and (b), but for frequency of averaged rainstorms (daily precipitation >100 mm).

(*qu*, *qv*) with statistical significance exceeding 10%. Figure 7a and 7b show that moisture transport pathways for the rainfall events with daily precipitation less than 500 mm are through westerly transport in the middle latitude, and southerly transport in the south of mainland China and coastal seas. The two pathways differ in their spatial scales as well as their locations. The vortex associated with rainstorms is smaller in size and located to the south (Figure 7a and 7b). The vortex associated with light-rainstorms (<50 mm) is larger in size and located to the north. In addition, for the rainstorms, in particular the extreme rainstorms (daily precipitation >100 mm), there is a region of high correlation oriented north-south from the northerly in the mid-latitudes to the west of the moisture transport vortex (Figure 7c and 7d). This indicates that moisture sources and transport pathways differ significantly for different rainfall categories, and for non-extreme rainfall and extreme rainfall events. The color-shaded region in Figure 7 indicates a statistically significant correlation between the column-integrated moisture fluxes and frequency of rainstorms in East China. Note that A and B denote statistically significant moisture transport flux components *qu* (Figure 7c) and *qv* (figure 7d), respectively. Our calculation indicates that the frequency of rainstorms and column-integrated moisture fluxes are significantly correlated; moisture sources of rainstorms in East China are the South China Sea and the Bay of Bengal. One branch originates from the South China Sea to the Bay of Bengal, deflecting to the southern border of the Tibet Plateau, and eventually turning to the rainstorm area in East China; the other branch is a direct moisture flow from the South China Sea to the rainstorm area in East China (not shown). The two moisture transport branches are modulated by active summer monsoonal flow and subtropical highs. Therefore, the correlation vector of moisture fluxes further confirms that moisture in the rainstorm area in East China mainly comes from the South China Sea and the western Pacific Ocean.

To further clarify the correlation between rainstorm frequency and moisture transport at those highly correlated regions, we use stepwise regression to select the predictors for frequency of extreme rainstorms (daily precipitation >100 mm) in East China in the four high correlation regions, A, B, C and D as shown Figures 7c and 7d. After statistical tests, the regression equation for interannual variation in the frequency of extreme rainstorms (Figure 8a) may be written as:

$$y = 0.002 \cdot qv_{\mathrm{A}} + 0.001 \cdot qv_{\mathrm{B}} - 0.001 \cdot qv_{\mathrm{C}} - 0.003 \cdot qv_{\mathrm{D}} + 0.306, \quad (4)$$

where y is the number of extreme rainstorms in East China, and qv_{A}, qv_{B}, qv_{C}, and qv_{D} are the average values of zonal and meridional moisture fluxes in the region A, B, C, and D, respectively. Statistical tests of the regression eq. (4) indicate that only the factors for meridional moisture flux are significant.

The results show that regressed values of interannual variation in the moisture flux for the frequency of extreme rainstorms in East China are in phase with the actual values, and the correlation coefficient between the two reaches 0.75 at the statistical significance level of 1%. This result also confirms that the occurrence of extreme rainstorms is closely related to the spatial structure of moisture flux in the high correlation region (Figure 8b). Multiple linear regression is also used for the rainstorms in the 50–99.9 mm category, and the regression equation is written as:

$$y = -0.002 \cdot qu_{\mathrm{B}} + 0.002 \cdot qv_{\mathrm{A}} + 0.003 \cdot qv_{\mathrm{B}} + 0.003 \cdot qv_{\mathrm{C}} - 0.008 \cdot qv_{\mathrm{D}} + 1.318, \quad (5)$$

where y is the number of rainstorms with daily precipitation between 50–99.9 mm, and other variables are defined as above. The A, B, C, and D regions are the same as in Figure 6c and 6d. Regression tests indicate that several zonal and meridional flux variables are statistical significant as predictors.

To further elucidate the relations between moisture transport and rainstorms in East China, we made a composite analysis based on a number of representative events in the years of higher rainstorm occurrence (1994, 1995, 1996, and 1998), and the years of lower rainstorm occurrence (1971, 1972, 1978, and 1989). The composite of column-integrated moisture flux in these two types of cases (Figure 9a and 9b) indicates that the anomalous moisture flux vectors show anticyclonic structure in East China during the years of lower occurrence, and cyclonic structure during the years of higher occurrence. This result reveals the circulation structure of moisture transport associated with rainstorms.

The grey arrows indicate the directions of moisture transport in anticyclonic or cyclonic circulations (dash cycles).

7. Moist flux vortices in the East Asia Monsoon, convergence, and interannual variations in summer rainstorms

We have shown that moisture transport and summer rainstorms in East China vary in phase and their correlation is statistically significant, and that moisture transport during extreme rainstorms under the influence of the summer monsoon is characterized by a vortex structure. We have also analyzed the merging of moisture transport pathways, and its characteristics during extreme rainstorm events. This section will further discuss whether or not the convergence of moisture pathways and the associated vortex structure closely related to extreme rainstorm events also show a similar north-south oscillation on the decadal time scale. Based on a correlation analysis between the zonal moisture flux and distribution of the regions with frequent moisture flux in East China, we ask the follow question: does the large-

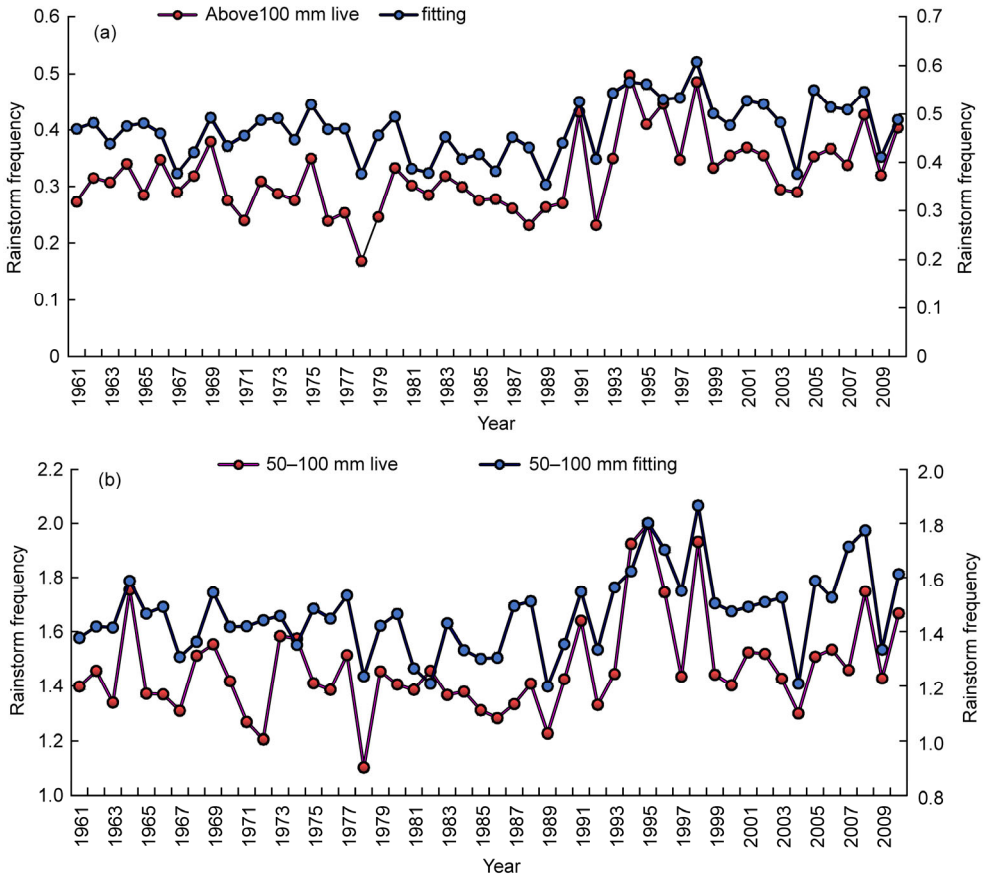

Figure 8 Interannual variations of rainstorm frequency (red curves) and its multiple regression (blue curves) for the rainstorm category. (a) Daily precipitation >100 mm; (b) daily precipitation between 50 and 100 mm.

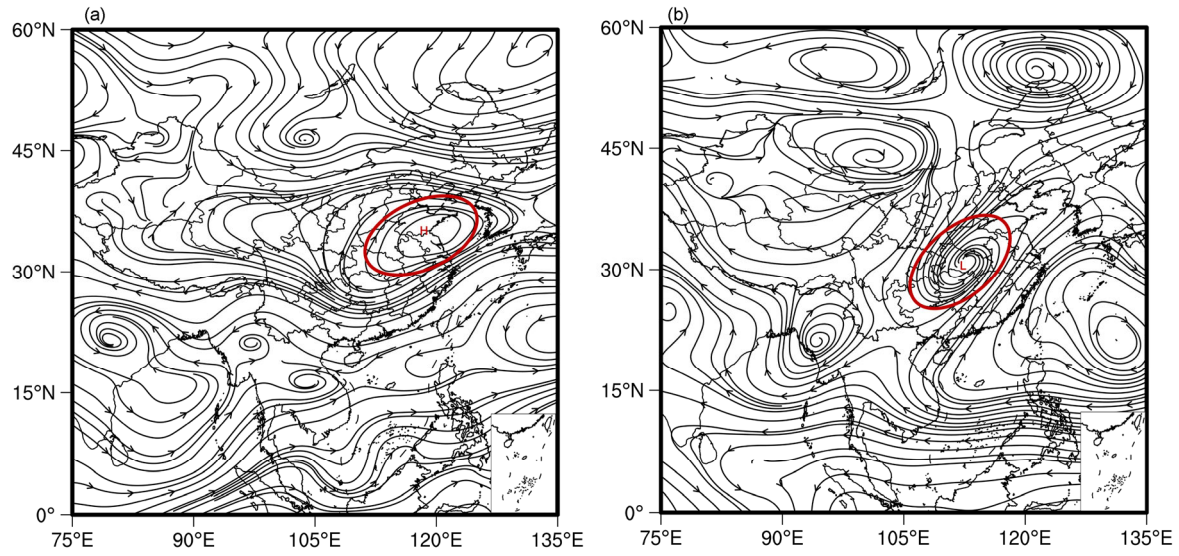

Figure 9 Streamlines of anomalous column-integrated moisture transport flux in the years of low (a) and high (b) rainstorm frequency with daily precipitation >50 mm.

scale moisture transport vortex also show north-south oscillation as does the region with frequent rainstorms in East China? Figure 10 depicts a time-latitude diagram of anomalous frequency of rainstorms (Figure 10a), vorticity anomaly (Figure 10b), and divergence anomaly (Figure 10c) averaged between 105°–120°E.

Figure 10 shows that the rainstorm frequency, the column-integrated moisture flux convergence anomaly, and the

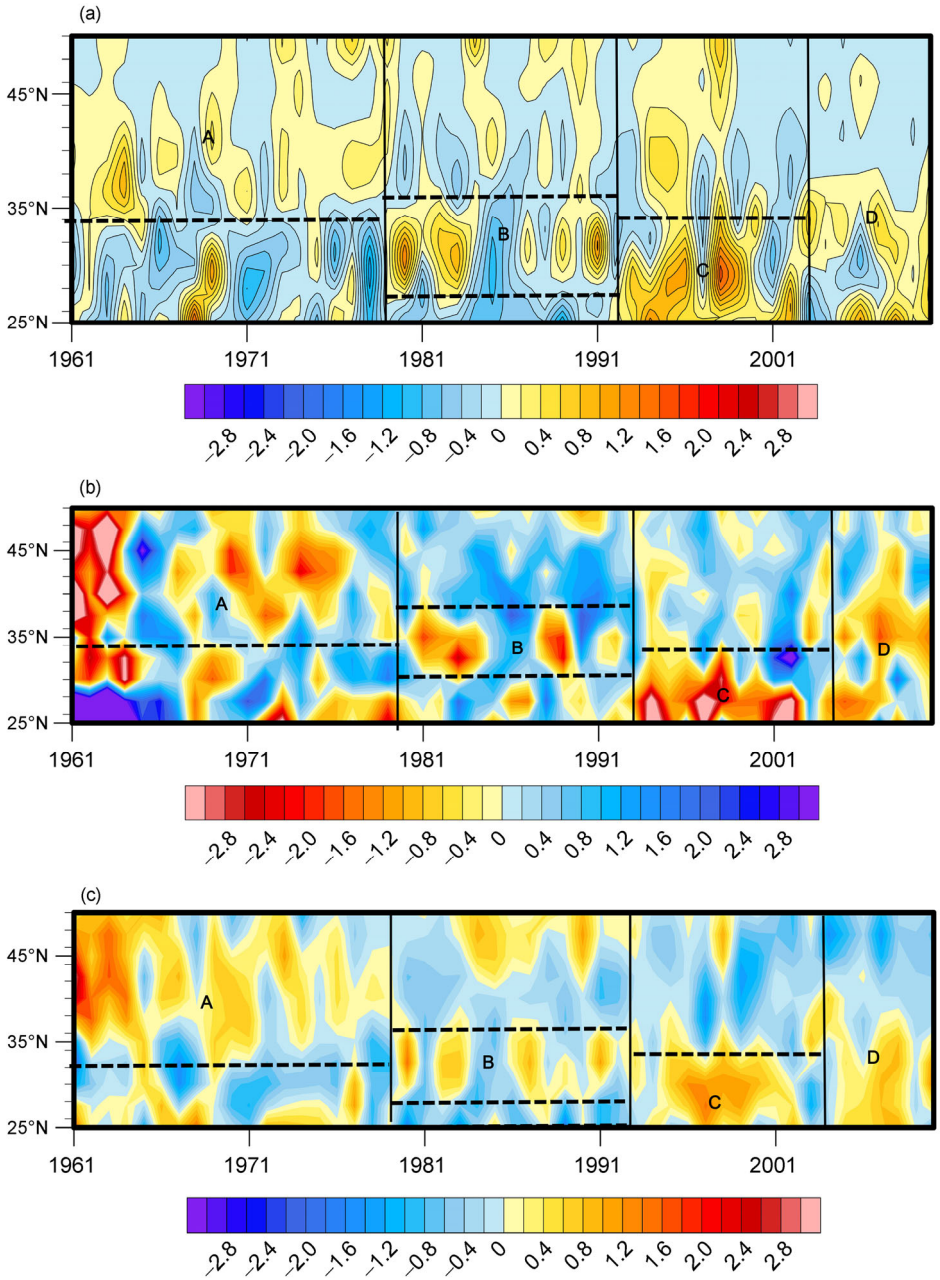

Figure 10 Time-latitude diagram of rainstorm frequency (a), divergence anomaly (b), and vorticity anomaly (c) averaged over 105°–120°E in East China from 1961 to 2010.

vorticity anomaly all vary in phase. Positive anomalies of rainstorms between 20°–50°N shift south at the decadal time scale (Figure 10a). High rainstorm frequency is found mostly in the north of this region in the 1960s (Figure 4bA), as is negative divergence (convergence) of the column-integrated moisture flux and positive anomaly of vorticity (Figure 10b and c). During the 1970s, more rainstorms are found to shift gradually south (Figure 4bB), and the same southward shifts are found for convergence of the column-integrated moisture flux and the positive anomaly of vorticity (Figure 10b and 10c). The southward trend continued through the 1980s (Figure 4bC). By the 1990s, the rainstorm area stays in the south (Figure 4bD), as do the other quantities (Figure 10b and 10c). During the 2000s, regions of frequent rainstorms remain generally stationary, with some signs of northward progression.

8. A conceptual model of moisture sources and moisture transport for rainstorms in East China

The recently developed method of Lagrangian particle tracking is a powerful tool to study moisture transport. Compared to Eulerian analysis, Lagrangian analysis has the

advantages of tracking the history of a cluster of pre-defined air particles, which makes it suitable for tracing the source regions of transported moisture. Wernli et al. (1997) first proposed that Lagrangian analysis could be used to track the transport of air parcels in the atmosphere, and that the change of specific humidity is approximately controlled by only two processes, evaporation and precipitation, from which one can identify water vapor equilibrium and transport. Real et al. (2001) and James et al. (2004) estimated the moisture sources of two extreme precipitation events, one in 1998 in the west of the Mediterranean sea, and the other in 2002 in Europe. It has also been demonstrated that Lagrangian analysis has the potential (Nieto et al., 2006) to be used to assess the relative contributions of different moisture sources (Sodemann et al., 2006).

To further verify the proposed conceptual model of moisture source and moisture transport for rainstorms in East China, we focus on the rainstorm events in the middle and lower reaches of the Yangtze River in 2008, which is one of the years with the highest occurrences of rainstorms. We use the Lagrangian analysis of moisture transport as the diagnostic tool (Chen et al., 2010). The 3D particle dispersion model FLEXPART is driven by the NCEP/NCAR reanalysis data. 3D backward trajectories of air particles are computed for the extreme precipitation events from 1 June to 9 June, and the data is used to calculate backward transport of air particles during this event. Figure 11a shows that the water vapor trajectories are characterized by the merging of three branches of moisture flow. One originates from the north of the Tibet Plateau and Loess Plateau, continuing to the south, making a "big bend" east of the plateaus, and eventually turning to the east. The second originates from the South China Sea, passing the Bay of Bengal, turning to the immediate south of the Tibet Plateau, and eventually moving to the rainstorm area in East China. The third also originates from the South China Sea, but moves directly to the rainstorm area in East China. The merging of the above three branches is the main characteristic of the moisture transport structure, and they eventually merge in the Yangtze River Valley. Results from our simulated moist air particles in this case study further confirm our prior conclusion on the structure of moisture transport to rainstorms in East China and the merging of different pathways.

Based on the above results, we synthesize a conceptual model of moisture transport pathways, vortices, and convergence for rainstorms in East China (Figure 11b; with the area of frequent rainstorms in the Yangtze River Valley and South China in the background). The column-integrated moisture transport pathways that constitute the merging structure in East China mainly originate from the east edge of the plateaus (qV_1), moisture flow from the Bay of Bengal, South China Sea, and Indochina Peninsula (qV_2, qV_3, qV_4), and they merge at the area of frequent extreme rainstorms in East China. Regions of statistically significant correlations between vorticity ($\Delta\zeta_{\max}$) and divergence ($\Delta D_{\max}$) and the column-integrated moisture flux coincide with the region of frequent summer rainstorms in East China. The high correlation region of the column-integrated moisture transport pathway ($IqvI_{max}$) in the concentrated rainstorm area is also collocated with the region of frequent summer rainstorms in East China. In addition, the frequent rainstorm area is situated in the merging area of multiple branches of cyclonic moisture transport pathways, characterized as a moisture transport vortex. Figure 11b illustrates the conceptual model of the moisture transport pathways, vortex pattern and divergence during extreme rainstorms in East China.

9. Conclusions

We have studied moisture transport and moisture flow patterns during rainstorm events in East China. Our main conclusions may be summarized as:

(1) Decadal variations of precipitation in East China are characterized by the pattern "flooding in the south and drought in the north". Precipitation in the west shows a slightly increasing trend. Decadal variation in precipitation in the Tibet Plateau and Loess Plateau and the transition zone to the eastern plain area are dominated by negative variations. Decadal variations in the frequency of rainstorms in the Tibet Plateau and Loess Plateau and the transition zone to the plain area differ from those of total precipitation in their characteristics, and show an increase in interannual variations (approximately similar positive and negative variation); frequency of mudslides increases in this region but shows no increase in western China. Geographical variations in the frequency of rainstorms in East China are consistent with the three-step staircase topography and the edge of the Meiyu system. The eastern region of the Tibet Plateau and Loess Plateau show an increase in the frequency of rainstorms. Northeast China shows an increase in interannual variations, the frequent rainstorm areas being oriented in the southeast-northwest direction (at the edge of high terrain) and gradually decreasing in that direction. Therefore, the interannual variations may be summarized as being "high in the southeast and low in the northwest", similar to the staircase topography.

(2) Interannual variations in total precipitation during the monsoon season in East China also show substantial differences from interannual variations in the frequency of extreme rainstorms. A comparison of total precipitation and frequency of rainstorms from 1961 to 2010 indicates that the two differ significantly in their phase in the interannual time scale, and have opposite decadal trends; i.e., the frequency of rainstorms has increased since the 1990s, while total summer precipitation decreases during the same period.

(3) The maximum moisture flux associated with summer precipitation events in East China is situated in the Yangtze-Huaihe River Valley, but it does not overlap with the maximum precipitation region, which is located in South China.

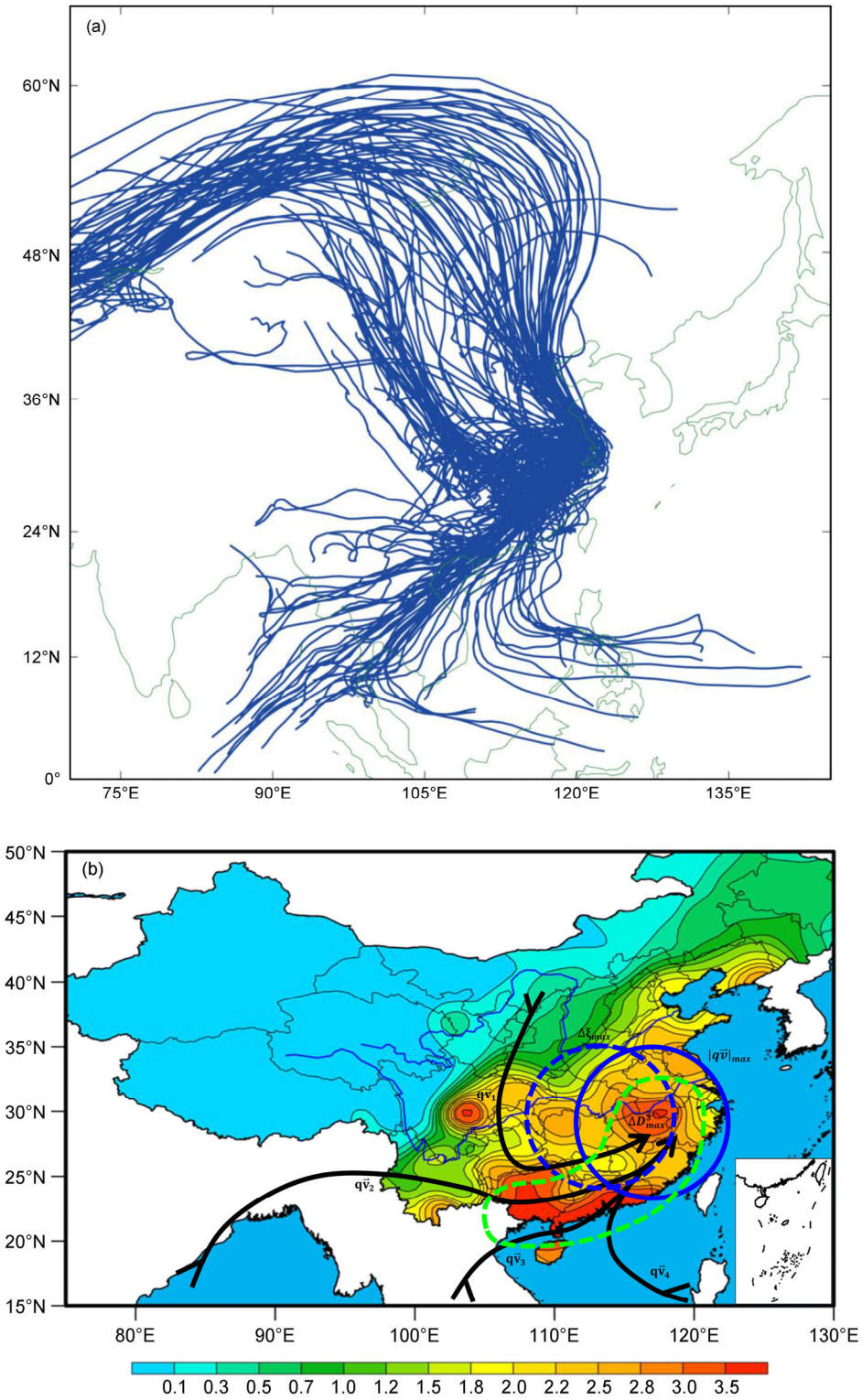

Figure 11 Backward trajectories of moist air particles associated with the rainstorms in East China (a), and diagram of the moisture transport (b). Black curves with arrows, *qv*1, *qv*2, *qv*3, *qv*4, represent the major transport routes of column-integrated water vapor; blue dotted and solid circles cover the regions with high correlations of vorticity ($\Delta\zeta_{max}$) and high divergence (ΔD_{max}) with column-integrated moisture transport flux to EC rainstorm frequency, respectively; the blue dashed circle marks the area of high correlation between column-integrated moisture transport flux ($|q\bar{v}|_{\max}$) and rainstorm frequency in East China. All correlation coefficients pass statistical tests at the significance level of 10%.

The maximum moisture flux associated with the area of frequent rainstorms is located in the south of the Yangtze River Valley, and overlaps with the area of frequent rainstorms itself. Transport pathways for non-storm precipita-

tion include moisture flow by westerlies and northwesterlies in the mid-latitudes, and the southerly moist flow from the south of the continent and offshore areas. The Yangtze River Valley and South China are both regions of high rainstorm frequency. Column-integrated moisture transport pathways to the area of rainstorm concentration may be described as a "merging" of three branches of intense moisture flow from the lower- and mid-latitude oceans, and this merging area is shifted slightly to the south in comparison to the maximum summer precipitation or non-rainstorm precipitation. For both non-storm precipitation and storm precipitation, frequency is correlated with the column-integrated moisture flux vector, i.e., moisture transport vortices with different spatial scales. Moisture transport vortices related to rainstorms are smaller in size, and located to the south; while the vortices not related to rainstorms are larger in size, and located to the south.

(4) Both the moisture transport vortex of column-integrated moisture flux and the convergence are important contributors to rainstorms in East China. It is shown that decadal variations of summer precipitation in East China and the frequency of rainstorms differ significantly in their spatial structure, and also differ in their moisture transport pathways, moist flow pattern, and in the merging area of moisture flows from the middle and low latitudes.

(5) It is shown that regions with highly frequent rainstorms in East China are changing dynamically on the interannual time scale, and this pattern is characterized by a south-north oscillation. This oscillation is synchronous on the decadal time scale with vorticity and divergence anomalies of the column-integrated moist flow under the influence of the changing summer monsoon. Finally, a conceptual model of moisture transport pathways for rainstorms in East China, moisture flow, and the vorticity and divergence structure are proposed to improve understanding of these extreme precipitation events.

Acknowledgements *We sincerely thank Dr. Hongwen Kang and Dr. Yanjun Wang at the Chinese Academy of Meteorological Sciences for providing data and references. This research was supported by the National Natural Science Foundation of China (Grant No. 41130960), the National Science and Technology Pillar Program of China (Grant No. 2012BAK10B04), and the National Department of Public Benefit Research Foundation of China (Grant No. GYHY201406001).*

References

Bao M, Huang R H. 2006. Characteristics of the interdecadal variations of heavy rain over China in the last 40 years (in Chinese). Chin J Atmos Sci, 6: 1057–1067

Chen B, Xu X D, Bian J C, Shi X H. 2010. Sources, pathways and timescales for the troposphere to stratosphere transport over Asian monsoon regions in boreal summer (in Chinese). Chin J Geophys, 53: 1050–1059

Chen L X, Zhu Q G, Luo H B. 1991. The East Asian Monsoons (in Chinese). Beijing: China Meteorological Press. 49–61

Chen S X. 1982. Definition and indexes of South China summer monsoon (in Chinese). Trop Geog, 2: 10–14

Chow K C, Tong H W, Chan J C L. 2008. Water vapor sources associated with the early summer precipitation over China. Clim Dyn, 30: 497–517

Church J, Clark P, Cazenave A, Gregory J, Jeverjeva S. 2014. Climate Change 2013: The Physical Basis: Contribution of Working Group Ⅰ to the Fifth Assessment Report of the Inter-government Panel on Climate Change. In: Stocker T, ed. UK: Cambridge University Press. 1135

Guo Q Y, Cai J N, Shao X, Sha W. 2003. Interdecadal variability of East-Asian summer monsoon and its impact on the climate of China. Acta Geographic Sin, 58: 569 –576

James P, Stohl A, Spichtinger N. 2004. Climatological aspects of the extreme European rainfall of August 2002 and a trajectory method for estimating the associated evaporative source regions. Nat Hazards Earth Syst Sci, 4: 733–746

Jin Z H. 1981. Moisture budget in the Hainan Area during the summer of 1979 (in Chinese). Proceedings of the National Conference on Tropical Summer Monsoon. Kunming: Yunnan People Publishing House. 151–164

Liu C Z, Wang H J, Jiang D B. 2004. The configurable relationships between summer monsoon and precipitation over East Asia (in Chinese). Chin J Atmos Sci, 28: 700–712

Liu Y Y, Ding Y H. 2009. Influence of the Western North Pacific summer monsoon on summer rainfall over the Yangtze River basin (in Chinese). Chin J Atmos Sci, 33: 1225–1237

Liu, X N. 1999. Climatic characteristics of extreme rainstorm events in China (in Chinese). J Catastroph, 14: 54–59

Ma Y, Chen W, Feng R Q, Liang J J, Liang Y Q. 2012. Interannual and interdecadal variations of precipitation over East China during Meiyu season and their relationships with the atmospheric circulation and SST (in Chinese). Chin J Atmos Sci, 36: 397–410

Nieto R, Gimeno L, Trigo R. 2006. A Lagrangian identification of major sources of Sahel moisture. Geophys Res Lett, 33: 273–274

Reale O, Feudale L, Turato B. 2001. Evaporative moisture sources during a sequence of floods in the Mediterranean region. Geophys Res Lett, 28: 2085–2088

Shen R G, Huang G S, 1981. On the relation between the monsoonal flow and moisture transport for precipitation in South China during the summer of 1980 (in Chinese). Kunming: Yunnan People Publishing House. 116–128

Shi N, Lu J J, Zhu Q G. 1996. East Asian winter/summer monsoon intensity indices with their climatic change in 1873-1989 (in Chinese). Trans Atmos Sci, 19: 168–177

Simmonds I, Bi D, Hope P. 1999. Atmospheric water vapor flux and its association with rainfall over china in summer. J Clim, 12: 1353–1367

Sodemann H, Palmer A S, Schwierz C, Schwikowski M, Wernli H. 2006. The transport history of two Saharan dust events archived in an alpine ice core. Atmos Chem Phys, 6: 667–688

Stohl A, Forster C, Frank A, Seibert P, Wotawa G. 2005. Technical note: The Lagrangian particle dispersion model FLEXPART version 6.2. Atmos Chem Phys, 5: 2461–2474

Tao J, Chen J K. 1994. Diagnosis of role of moisture sources and passages in Meiyu raingush genesis (in Chinese). Trans Atmos Sci, 17: 443– 447

Tao S Y, Zhu W M, Zhao W. 1988. Interannual variability of Meiyu rainfalls (in Chinese). Chin J Atmo Sci, 12: 13–21

Tao S Y. 1980. Heavy Rainfalls in China (in Chinese). Beijing: Science Press. 1–3

Tian H, Guo P W, Lu W S. 2002. Features of water vapor transfer by summer monsoon and their relations to rainfall anomalies over China (in Chinese). J Nanjing Inst Meteor, 25: 496–502

Wang H J. 2001. The weakening of the Asian monsoon circulation after the end of 1970's. Adv Atmos Sci, 18: 376–386

Wang S, Gong D. 2000. Climate in China during the four special periods in Holocene. Prog Nat Sci, 5: 379–386

Wang S W, Ca J N, Zhu J H, Gong D Y. 2002. The Interdecadal variation of annual precipitation in China during 1880s–1990s (in Chinese). Acta Meteorolog Sin, 60: 637–639

Wernli H, Davies H C. 1997. A Lagrangian-based analysis of extratropical cyclones. I: The method and some applications. Q J R Meteorol Soc, 123: 467–489

Xu X D, Shi X Y, Wang Y Q, Peng S Q, Shi X H. 2008. Data analysis and

numerical simulation of moisture source and transport associated with summer precipitation in the Yangtze River valley over China. Meteorol Atmos Phys, 100: 217–231

Xu X, Lu C, Ding Y, Shi X, Guo Y, Zhu W. 2013. What is the relationship between China summer precipitation and the change of apparent heat source over the Tibetan plateau. Atmos Sci Let, 14: 227–234

Xu X, Lu C, Shi X. 2010. Large-scale topography of China: A factor for the seasonal progression of the Meiyu rainband. J Geophys Res, 115: 355–365

Zhao H, Zhang R H, Wen M, 2015. Severe rainfalls in South China during May 2013 and its relation to the onset of the South China Sea summer monsoon (in Chinese). Acta Meteorolog Sin, 73: 442–458

Zhou Y S, Gao S T, Deng G, 2005. A diagnostic study of water vapor transport and budget during heavy precipitation over the Yangtze River and the Huaihe River basins in 2003 (in Chinese). Chin J Atmos Sci, 29: 195–204

Zhu Q G. Principle of the Synoptic Meteorology and Methods (in Chinese, the fourth edition). Beijing: China Meteorological Press. 321–323